Experiment 3.36:
The Cahn – Hillard Equation: Computer Simulations and Analytical Investigations

Alireza Haghpanah Jahromi (2524241)
Ege Semercioglu (2787745)

Supervisor: Kay-Robert Dormann

Date: 15.07.2024

TECHNISCHE UNIVERSITÄT DARMSTADT

Advanced physics lab course

Section B

Department of Condensed Matter

Declaration of independent elaboration:

We hereby assure that we have prepared this elaboration of the experiment without the help of third parties and only with the specified sources and aids. All passages taken from sources are marked as such. This work has not yet been submitted to any examination authority in the same or a similar form.

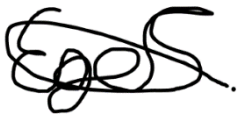

Ege Semercioglu

Alireza Haghpanah Jahromi

Contents

Aim of the study

The aim of this study is to comprehensively investigate the dynamics of phase separation in binary mixtures using both analytical and numerical approaches within the framework of the Cahn-Hilliard equation. The study analyzes steady-state solutions of the Cahn-Hilliard equation to predict phase boundaries, like spinodal and binodal lines, in two-component systems. By combining the Cahn-Hilliard model with Flory-Huggins theory, it explores phase separation dynamics and spatial structures. By constructing a state diagram, the research will map out the conditions under which different phases form, providing a deeper understanding of the equilibrium and non-equilibrium behavior of mixtures. The numerical simulations will be employed to explore the influence of key parameters such as timestep, system size, and resolution on the phase separation process, ensuring that density is conserved and the evolution of phase interfaces is accurately captured. These simulations will also be used to validate theoretical predictions, particularly by examining the spinodal region and metastable regimes, to verify the consistency between analytical and numerical results. Furthermore, the study will investigate the long-term dynamics of phase-separated structures by simulating large systems, analyzing the growth of domains, and calculating structure factors to determine the growth exponent in the phase-separating regime. This comprehensive approach aims to shed light on the kinetics and morphology of phase separation, offering valuable insights into the behavior of non-reactive binary mixtures and the broader field of non-equilibrium phenomena in condensed matter physics.

1 Introduction

Phase separation is a fundamental phenomenon in condensed matter physics and materials science, manifesting when a homogeneous mixture of two or more components separates into distinct regions with different compositions. This process is commonly observed in systems such as oil and water mixtures, polymer blends, and alloys. The Cahn-Hilliard equation provides a powerful theoretical framework for understanding the dynamics of phase separation, in non-reactive binary mixtures where the composition remains time-independent. Unlike classical thermodynamic approaches, which primarily address equilibrium properties, the Cahn-Hilliard equation models the temporal evolution of phase separation, capturing key processes such as nucleation, growth, and the coarsening of domains. The motivation for studying phase separation dynamics stems from its widespread relevance in natural and industrial processes. For example, the formation of microstructures in alloys, the development of patterns in biological tissues, and the behavior of complex fluids all involve phase separation phenomena. Understanding these dynamics can lead to advancements in material design, where controlling the microstructure is crucial for tailoring properties such as mechanical strength, conductivity, and optical behavior. This study specifically focuses on the Cahn-Hilliard equation, which extends traditional thermodynamic models by incorporating the effects of spatial inhomogeneity and conserved dynamics. The equation is derived from a free energy functional that includes contributions from both the local composition and its spatial gradients, thereby accounting for the interfacial energy between phases. This formulation allows for the investigation of phase separation not just as a final state, but as a dynamic process where the interface between phases evolves over time. In this work, we aim to explore phase separation both analytically and numerically. The analytical approach will involve deriving steady-state solutions of the Cahn-Hilliard equation and using these solutions to predict phase boundaries, such as the spinodal and binodal lines, which delineate regions of stability and instability in the phase diagram. Numerical simulations will complement this by examining how factors like timestep, system size, and resolution affect the accuracy of phase separation dynamics. By simulating large systems over extended periods, we will also analyze the growth of domains and the structure factors, ultimately determining the growth exponent that characterizes the phase-separating regime.

Overall, this study seeks to provide a comprehensive understanding of phase separation dynamics in binary mixtures, offering insights that could be applied to various fields, from materials science to biological systems. The combination of analytical predictions with numerical simulations will help validate theoretical models and enhance our understanding of the complex, often nonlinear, processes governing phase separation. Additionally, the Flory-Huggins theory will be referenced to provide a deeper understanding of the thermodynamics involved in polymer blends and solutions. This theory is crucial for describing the mixing behavior of polymers, taking into account the entropy of mixing and the interaction parameter between different components. By incorporating the Flory-Huggins theory, we can better predict the conditions under which phase separation occurs in polymer systems, as well as the resulting microstructures. This theoretical framework complements the Cahn-Hilliard equation by offering insights into the molecular interactions and energetic considerations that drive phase separation, thereby providing a more comprehensive picture of the process.

2 Theoretical Principles

2.1 Theoretical Foundations of Phase Separation:

In this section, we delve into the thermodynamic and kinetic principles underlying equilibrium phase separation in binary mixtures, beginning with the Flory-Huggins theory. This theory, developed independently by Paul Flory and Maurice Huggins in the 1940s, provides a framework for understanding whether a binary mixture will remain homogeneous or separate into distinct phases [1]. The Flory-Huggins model conceptualizes the system as a lattice with N_0 sites, each of equal volume V_A, occupied by particles of species A and B. The concentration of species A in the lattice, denoted as ϕ_A, is given by the ratio $\phi_A = \frac{N_A}{N_0}$, where N_A is the number of particles of type A. The entropy of the system, which is a measure of the number of possible configurations, can be expressed as $S = K_B \ln W$, where W is the number of configurations and K_B is the Boltzmann constant [2].

To simplify the analysis, Stirling's approximation is applied, leading to the expression $S = const - K_B N_0[(1-\phi_A)\ln(1-\phi_A) + \phi_A ln\, \phi_A]$. This expression accounts for the translational entropy of the atoms. However, in a binary system, interactions between adjacent atoms must also be considered. These interactions are characterized by the Bragg-Williams model, which describes the energy associated with pairs of neighboring sites, depending on whether they are occupied by A-A, B-B, or A-B pairs. The internal energy of the system is then given by $U = \epsilon_{AA}N_{AA} + \epsilon_{AB}N_{AB} + \epsilon_{BB}N_{BB}$ where $\epsilon_{AA}, \epsilon_{AB}, \epsilon_{BB}$ are the interaction energies for A-A, A-B, and B-B pairs, respectively.

In a large lattice with a coordination number C , which represents the number of nearest neighbors each site has, the total number of bonds is $\frac{C \cdot N_0}{2}$. For species A, the number of bonds involving A atoms is given by $C \cdot N_A = 2N_{AA} + N_{AB}$, and similarly for species B. The total free energy F of the system is derived by considering both the internal energy and the entropy, resulting in the equation:

$$F = U - TS = F_0 + N_0 \frac{C}{2}\left(\epsilon_{AB} - \frac{1}{2}\epsilon_{AA} - \frac{1}{2}\epsilon_{BB}\right)\phi(1-\phi) + K_B T N_0[(1-\phi)\ln(1-\phi) + \phi \ln\phi]$$

Here, F_0 represents the free energy of the pure components before mixing. The interaction parameter $\boldsymbol{\chi}$, crucial for determining the tendency towards phase separation, is defined as:

$$\chi = \frac{C}{2K_B T}\left(\epsilon_{AB} - \frac{\epsilon_{AA} + \epsilon_{BB}}{2}\right)$$

The free energy of mixing has three components: an interaction term influenced by $\boldsymbol{\chi}$, which can be positive, negative, or zero, and two entropy terms that always favor mixing. If $\boldsymbol{\chi} > 0$, the system shows a tendency towards phase separation, whereas $\boldsymbol{\chi} \leqslant 0$ suggests a homogeneous mixture.

Further, the spindoal curve is introduced as a critical concept in phase diagrams, representing the boundary beyond which a single-phase mixture becomes unstable (Variations in composition will result in the natural separation of phase) . This curve is determined by the condition where the second derivative of the free energy with respect to composition becomes zero.

$$\frac{\partial^2 F}{\partial \phi^2} = 0$$

Differentiating the free energy expression twice with respect to ϕ we get:

$$\frac{\partial^2 F}{\partial \phi^2} = \frac{1}{\phi(1-\phi)} - 2\chi$$

Setting this equal to zero at the spinodal gives the critical value of χ at spinodal decomposition, χ_s:

$$\frac{1}{\phi(1-\phi)} = 2\chi_s$$

The interaction parameter at the spinodal, $\boldsymbol{\chi}_s$, can be calculated as:

$$\chi_s = \frac{1}{2}\left(\frac{1}{\phi} + \frac{1}{1-\phi}\right)$$

At the lowest point on the (ϕ,$\boldsymbol{\chi}$)-plane, known as the critical point, the instability first appears, characterized by $\phi_c = \frac{1}{2}$ and $\chi_c = 2$. This critical point marks the onset of spontaneous phase separation within the spinodal region, where any composition fluctuation leads to a decrease in free energy and, consequently, phase separation. The phase diagram, including the spinodal and binodal curves, visually represents these regions of stability, instability, and metastability, guiding our understanding of phase behavior in binary mixtures.

2.1 Binodal Curve:

According to Gibbs' phase rule, a two-component system can exhibit at most two coexisting liquid phases during phase separation [1]. When such separation occurs, the system divides into two distinct phases: one that is rich in component A and one that is poor in A, or conversely, rich in B and poor in B. The initial conditions of the system are crucial, as they determine the concentration distribution, which in turn influences the evolution of phase separation. In the context of binodal phase separation, the system typically begins with a homogeneous or slightly perturbed concentration profile. As the interaction parameter χ increases beyond the spinodal threshold, spinodal decomposition occurs, leading to a reduction in free energy with minor concentration changes, while still conserving the total number of monomers.

The binodal curve represents the boundary where phase separation becomes energetically favorable (there can be exceptions depending on the specific system and conditions. For example: In some cases, a system can remain in a metastable state even within the binodal region, delaying phase separation. High kinetic barriers can prevent or slow down phase separation, even if it is energetically favorable. In multicomponent systems, interactions between different components can lead to deviations from the expected behavior). It is defined by the condition that small local changes in concentration increase the system's free energy, but larger changes can lead to a more stable phase-separated state. This curve can be calculated by taking the derivative of the free energy with respect to the concentration ϕ and setting it to zero, leading to the binodal expression:

$$\frac{\partial F(\phi,\chi)}{\partial \phi} = 0$$

This results in the binodal condition:

$$\chi_b = \frac{1}{2\phi - 1}\ln\left(\frac{\phi}{1-\phi}\right)$$

The binodal and spinodal curves intersect at the critical point of the phase diagram. Below this critical point $\chi < \chi_c$, the system remains stable across the full concentration range $0 \leqslant \phi \leqslant 1$. However, when $\boldsymbol{\chi}$ exceeds the critical value $(\chi > \chi_c)$, a metastable region emerges between the spinodal and binodal curves. In this region, the equilibrium state is characterized by two phases with distinct compositions $\phi'$and ϕ'', corresponding to the branches of the coexistence curve at a given $\boldsymbol{\chi}$.

To bridge the Flory-Huggins free energy model with the Cahn-Hilliard equation, we can expand the free energy function around the critical point $(\boldsymbol{\chi}, \phi)$ = (2, 1/2). For a symmetric 1:1 mixture, where the uniform phase is ϕ = ϕ_0 = 1/2 , the free energy can be expanded up to the fourth order:

$$F = k_B T N \left[\frac{\chi}{4} - ln2 + (2-\chi)\left(\phi - \frac{1}{2}\right)^2 + \frac{4}{3}\left(\phi - \frac{1}{2}\right)^4\right]$$

In this expansion, the first two terms are constants and do not contribute to the phase separation process. The remaining terms capture the essential physics of phase separation, particularly near the critical point, by relating the composition fluctuations to the system's free energy landscape.

2.3 Spatial Dynamics:

Landau Mean-Field Theory:

The Landau mean-field theory proposes that a system evolves in such a way that it minimizes its free energy functional, F[ϕ(x)] . Here, ϕ(x) is represents an order parameter field near the critical point. The free energy functional is expressed as an integral over the system's volume, V :

$$F[\phi(x)] = \int_v f(\phi(x), \nabla\phi(x) dx$$

The free energy density f can be decomposed into a homogeneous part, f_{hom}, and an inhomogeneous part, f_{inhom}. The homogeneous part can be expanded around the critical point ϕ_0 to the fourth order as $f_{hom} = \frac{a}{2}\phi^2 + \frac{b}{4}\phi^4$ The linear term is omitted as it does not significantly impact the results, and the cubic term is excluded to simplify the analysis, as it complicates the algebra without adding much physical insight. The inhomogeneous part accounts for the energy cost associated with the gradient of the order parameter, which is significant at interfaces between phases. This contribution is represented as $f_{inhom} = \frac{k}{2}(\nabla\phi)^2$. Thus, the overall free energy density is given by:

$$f = \frac{a}{2}\phi^2 + \frac{b}{4}\phi^4 + \frac{k}{2}(\nabla\phi)^2$$

This formulation links to the Flory-Huggins theory by re-expressing the order parameter ϕ as $\tilde{\phi} = 2\phi - 1$, leading to a free energy expression similar to the one derived earlier. However, the term associated with the gradient of the order parameter (which penalizes interface formation) cannot be captured by the Flory-Huggins theory, as it does not account for spatial inhomogeneities. The coefficients can be identified as $a = 2k_BTN$ and $b = \frac{16\,k_BTN}{3}$.

Conserved Dynamics (Mean-Field Model B):

For systems with non-reacting components, where total mass and concentration are conserved, we use the mean-field Model B to describe the dynamics. The conservation of the order parameter ϕ implies that its dynamics must obey a continuity equation:

$$\dot{\phi}(\vec{x},t) + \nabla \cdot \vec{j}(\vec{x},t) = 0$$

Here, $\vec{j}(\vec{x},t)$ is the flux representing the net motion of the components. This flux occurs only in regions where the system is not locally in equilibrium, i.e., where $\delta F/\delta\phi = 0$. The simplest form of this flux is $\vec{j} = -M\nabla\delta F/\delta\phi$, where M is a mobility coefficient with dimensions of a diffusion coefficient. Combining these elements yields the mean-field Model B equation:

$$\dot{\phi}(\vec{x},t) = \boldsymbol{\nabla}.[M\nabla\frac{\delta F\,[\phi(\vec{x},t)]}{\delta\phi}]$$

Cahn-Hilliard Equation:

To model the dynamics of phase separation, we apply Model B to the free energy functional derived earlier, resulting in the Cahn-Hilliard equation. This equation, a nonlinear partial differential equation, describes the evolution of the conserved order parameter ϕ:

$$\dot{\phi}(\vec{x},t) = \boldsymbol{\nabla}.[M\nabla(a\phi + b\phi^3 - k\nabla^2\phi)]$$

For binary mixtures, ϕ corresponds to the local concentrations of the components. To simplify, we can nondimensionalize the equation by selecting appropriate units of length x_u and time t_u, leading to:

$$\frac{\partial\phi}{\partial t'} = \nabla' \cdot [\nabla'\left(\frac{Mt_u a}{x_u^2}\phi + \frac{Mt_u b}{x_u^2}\phi^3 - \frac{Mt_u k}{x_u^4}\nabla'^2\phi\right)]$$

By choosing $\frac{Mt_u b}{x_u^2} = 1$ and $\frac{Mt_u k}{x_u^4} = 1$, we define the characteristic length and time scales as $x_u = \sqrt{k/b}$ and $t_u = k/Mb^2$. This allows us to express the equation in a dimensionless form:

$$\dot{\phi}(\vec{x},t) = \boldsymbol{\nabla}.[\nabla(\alpha\phi + \phi^3 - \nabla^2\phi)]$$

where $\alpha = \frac{a}{b}$ is a dimensionless parameter. This form of the Cahn-Hilliard equation is used to describe the dynamics of phase separation in binary mixtures, capturing the evolution of concentration fields over time [3].

3. Results

Interface Profile Analysis:

We employed the Equation 3.1 to analyze the interface profile between two phases in our one-dimensional system at equilibrium:

(3.1) $$\phi(x) = \sqrt{-\frac{a}{b}}\tanh\left(\sqrt{-\frac{a}{2\kappa}}x\right)$$

$$Alpha = \frac{a}{b}$$

where 'a' relates to the free energy well depth, 'b' represents the free energy well curvature near the minima, and 'κ' is the interfacial energy parameter controlling interface width.

Parameter Fitting Results:

As Figure 3.1 and Figure 3.2 represent scaling behaviour, with Equation 3.1, fitted values of alpha(a/b) are compared against their theoretical expectations using scaling plots:

1. Parameter 'alpha': The plots showed a generally linear trend along y=x, indicating close alignment between fitted and expected values. Minor deviations were observed, potentially due to numerical inaccuracies or specific initial conditions.

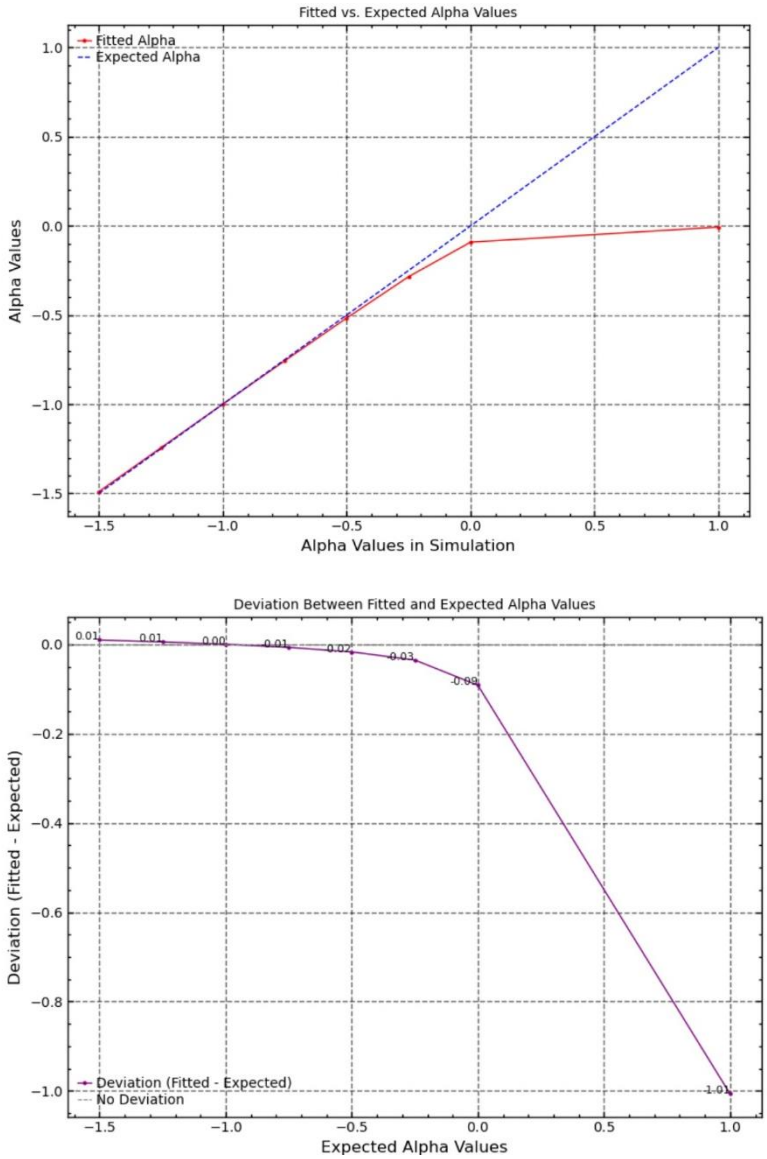

Figure 3.1 Scaling plots with fitted values

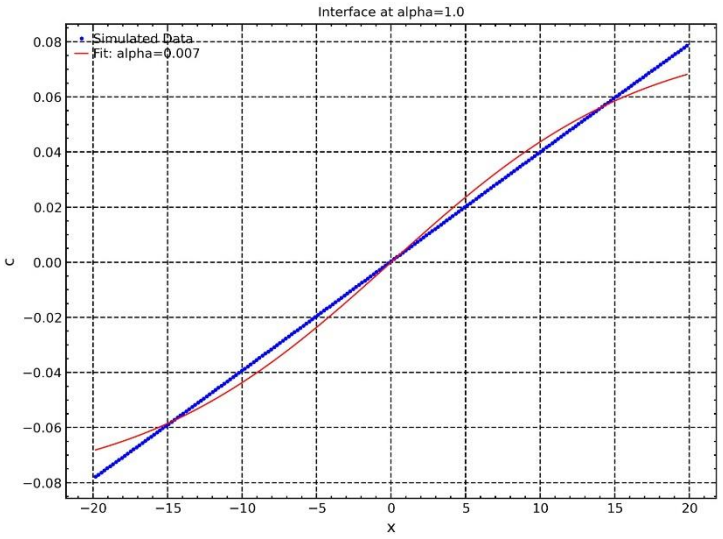

Alpha 1

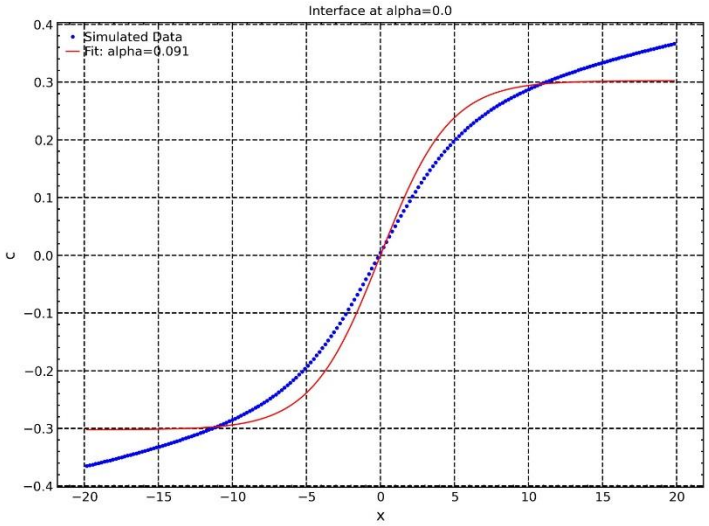

Alpha 0

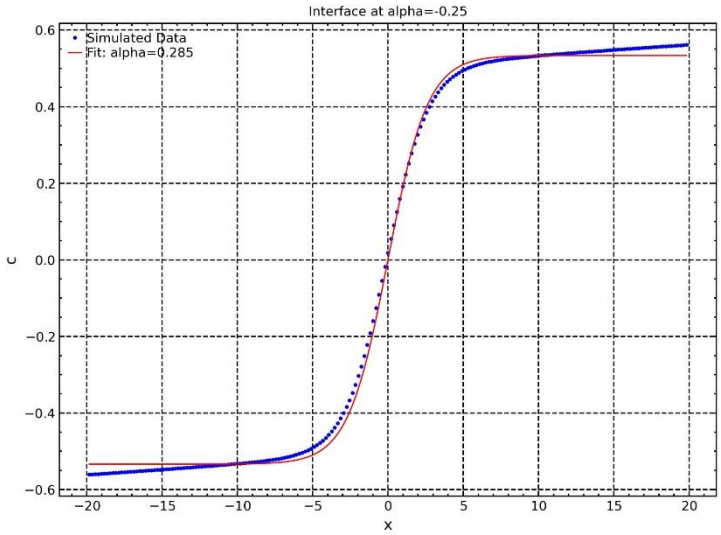

Alpha -0.25

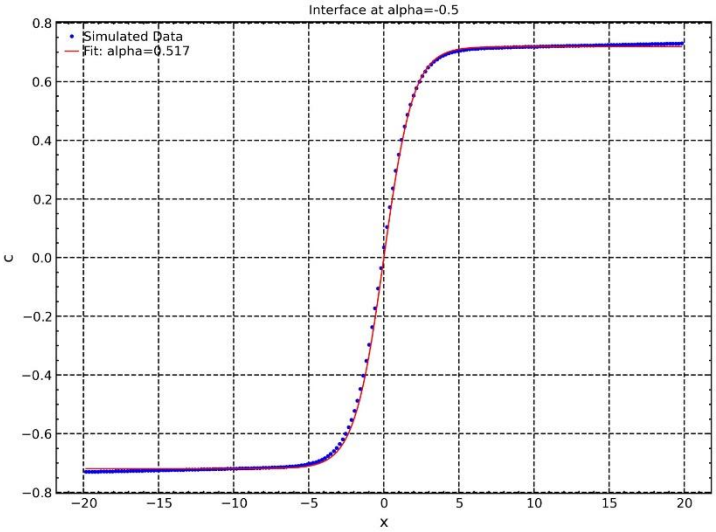

Alpha -0.5

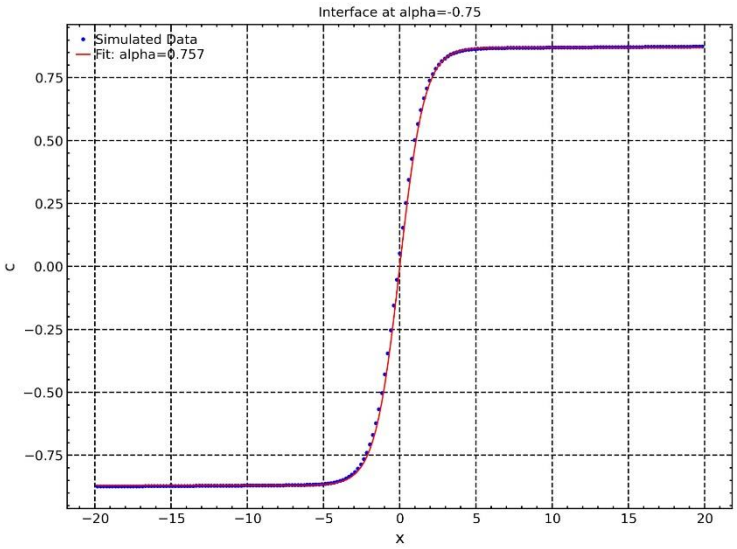

Alpha -0.75

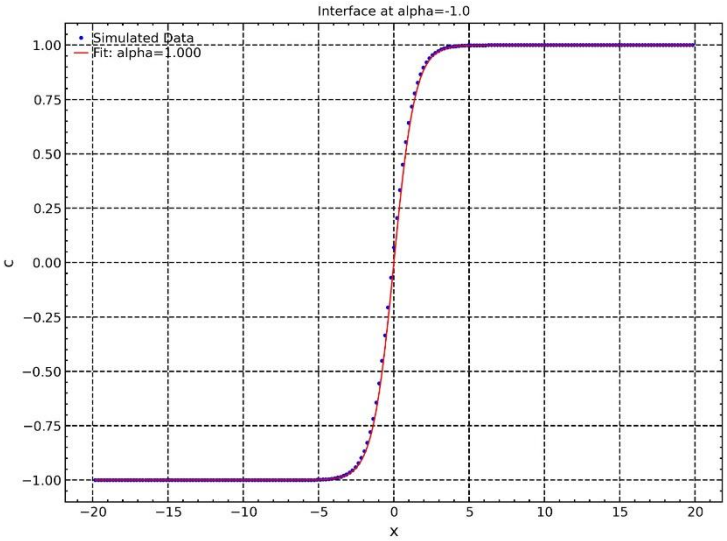

Alpha -1

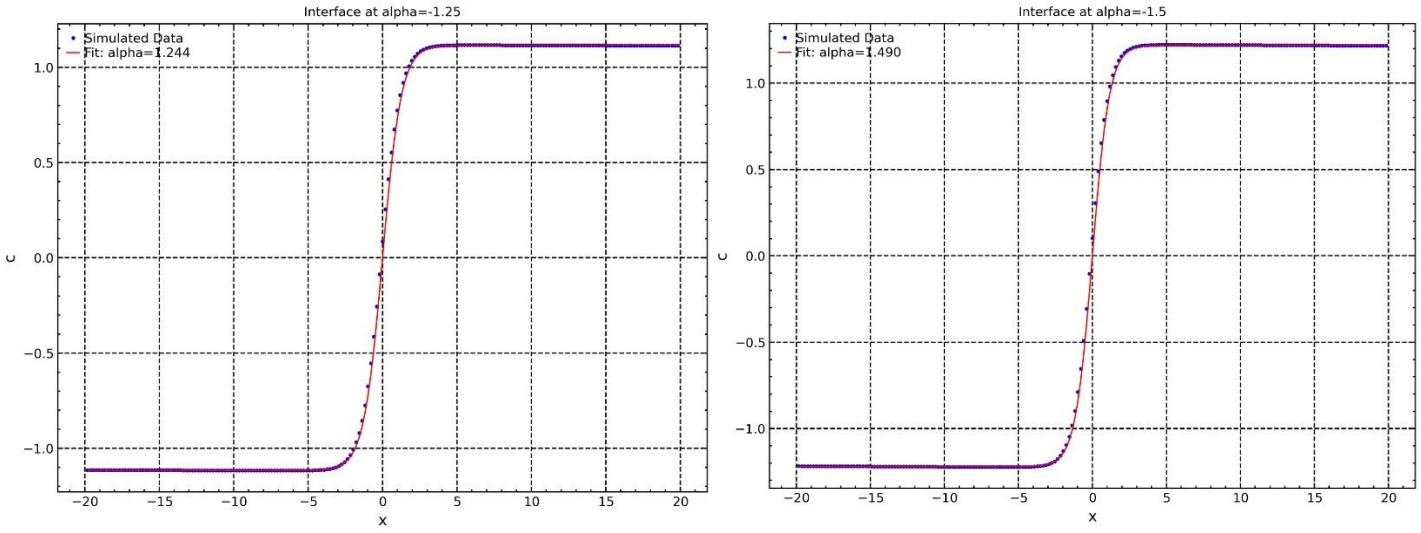

Alpha -1.25 **Alpha -1.5**

Figure 3.2 Fits diagrams for different interfaces at alpha values.

When observing the interface simulations, it becomes evident that there is no distinct interface for alpha values of 0 and 1. However, starting from alpha = -0.5, and then progressing to -0.75 and -1, a smooth interface emerges with increasing time steps, potentially indicating phase separation. We will analyze and refine these observations by conducting a linear stability analysis on the simulation data and comparing the results.

We automated the linear stability analysis using Python and AMEP. According to the Cahn-Hilliard framework and the state diagram provided in the Figure 3.3, the numerical results align well with the predictions made by linear stability analysis concerning phase separation. The state diagram plots the parameter alpha, likely related to interaction strength, on the y-axis, and composition (phi) on the x-axis. The red dots indicate regions where phase separation occurs, while the blue dots signify regions where no phase separation is observed.

Linear stability analysis predicts the conditions under which spinodal decomposition is expected, typically constrained by specific values of composition and parameters such as alpha. According to the Flory-Huggins theory and the Cahn-Hilliard model, spinodal decomposition occurs when the second derivative of the free energy curve is negative-which is inside the spinodal region according to definition of spinodal- and signaling instability.

The graph clearly delineates the regions of phase separation from those without it. The phase boundary aligns with theoretical predictions, as phase separation occurs at certain critical values of alpha and composition (phi), corresponding to the red dots. The critical points derived from linear stability analysis, as represented by the dashed green lines, appear to match the boundaries between phase-separated and non-phase-separated regions in the simulation.

This agreement between the predicted spinodal region and the simulation results, indicated by the red and blue dots, suggests strong consistency between the theoretical analysis and the numerical outcomes. If discrepancies were present (although none are evident in this graph), they could be attributed to numerical approximation errors, such as discretization limitations or deviations caused by non-linear effects beyond the scope of the initial linear stability predictions. Additionally, assumptions in the derivation of the Cahn-Hilliard equation may not fully capture the complex dynamics seen in simulations. Nonetheless, the graph demonstrates excellent agreement between the numerical and analytical results.

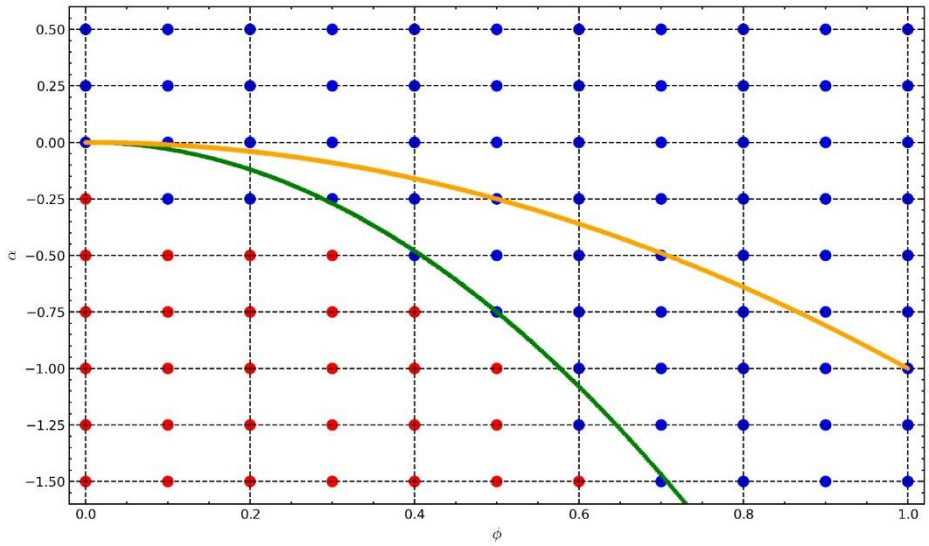

Figure 3.3 The state diagram shows regions of phase separation (red dots) and no separation (blue dots) as a function of alpha (y-axis) and composition phi (x-axis), with green dashed lines marking critical values. Also, the green line shows the spinodal line $\boldsymbol{\phi^2 = -\alpha/3}$ and the yellow one is binodal line $\boldsymbol{\phi^2 = -\alpha}$

We extracted these functions from the free energy functional of Landau theory, as we wrote in section 2.3 expressed as

$\boldsymbol{f = \frac{a}{2}\phi^2 + \frac{b}{4}\phi^4 + \frac{k}{2}(\nabla\phi)^2}$ to find the binodal line, we set the first derivative of the functional with respect to zero, which corresponds to finding the equilibrium states where the free energy is minimized which expressed as

$\boldsymbol{\frac{\partial f(\phi)}{\partial \phi} = a\phi + b\phi^3 - k(\nabla\phi)(\nabla\phi)' = 0}$ in homogeneous systems $\boldsymbol{k(\nabla\phi)(\nabla\phi)' = 0}$ **,** so we can continue with solving the homogeneous part of the equation and set the parameter $\boldsymbol{\alpha = a/b}$ which leads to $\boldsymbol{\phi^2 = -\alpha}$ for the binodal line. To find the spinodal line, we set the second derivative with respect to ϕ to zero. This identifies the limit of stability of the homogeneous phase which leads to $\boldsymbol{\frac{\partial^2 f(\phi)}{\partial \phi} = a + 3b\phi^2 = 0}$ and $\boldsymbol{\phi^2 = -\alpha/3}$

As an example, Figure 3.4 shows The Cahn-Hilliard simulation results presented in the next images demonstrate the spatial evolution of phase separation for varying alpha and phi values at 10000th timestep, which one can check the predictions of linear stability analysis. The simulation is visualized through 2D contour plots with a color scale spanning from -1 (dark purple) to +1 (yellow), representing the distinct separating phases within a 50x50 unit domain. The phase separation process -inside the spinodal region- exhibits characteristic spinodal decomposition behavior, where the initially mixed components spontaneously separate into well-defined domains. For the points that phase separation occurs, as the simulation progresses from t =0 to t = 2000, the system undergoes continuous evolution, beginning with initial separation featuring small, irregular domains, followed by domain coarsening and the formation of increasingly larger, circular structures. The interface between phases displays a smooth gradient (indicated by green-blue transition regions), which is a hallmark of the Cahn-Hilliard diffuse interface model. The circular morphology of the domains reflects the system's tendency to minimize interfacial energy, a fundamental characteristic of spinodal decomposition in systems governed by the Cahn-Hilliard equation. This temporal evolution from early-stage separation to the final stable configuration demonstrates the classic behavior of phase separation dynamics, with the system progressively organizing into well-defined, energetically favorable domain structures.

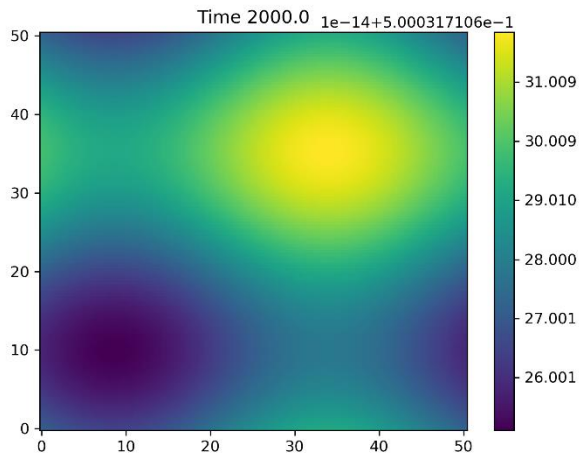

a

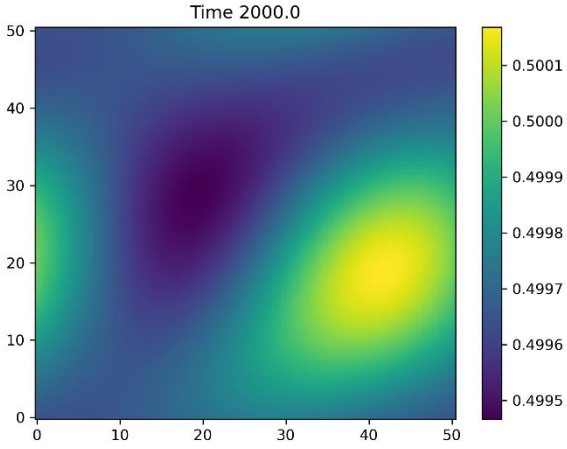

b

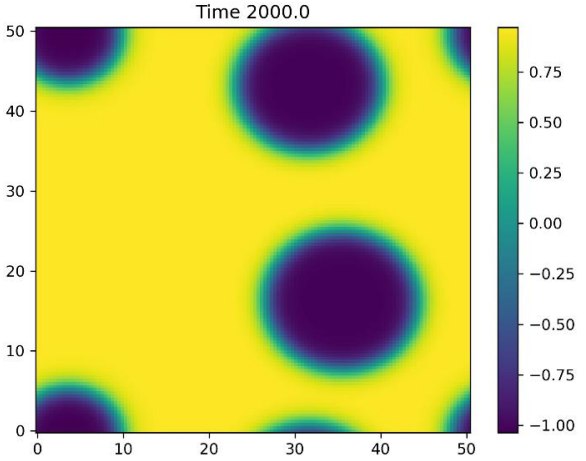

c

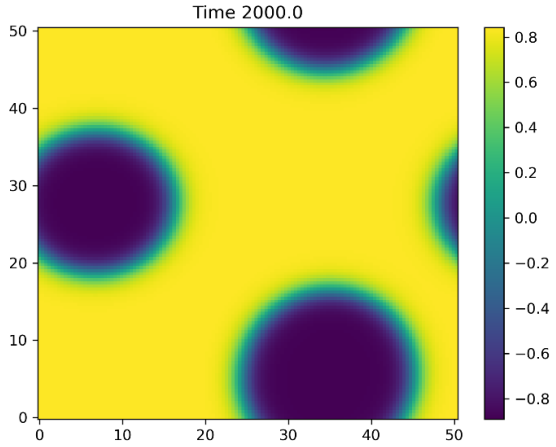

d

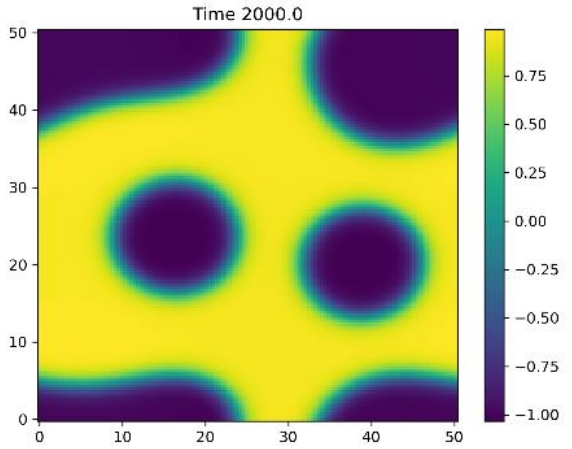

e

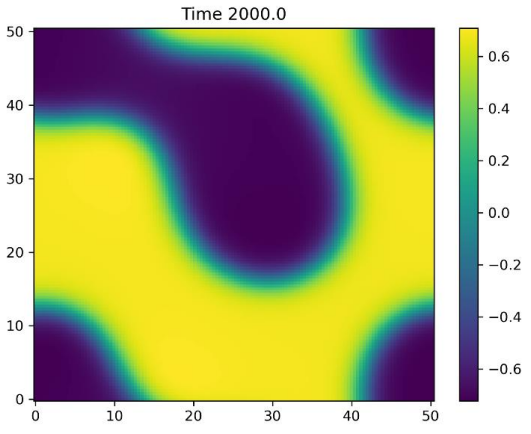

f

Figure 3.4 Simulation results for varying points; following, first value indicates alpha and second value composition phi: a)0, 0.5, b)-0.75, 0.5, c) -1, 0.5, d)-0.75, 0.4, e) -1, 0.2, f)-0.5, 0.1.

The spinodal line is likely positioned within a narrow boundary between the blue and red dots. Above this boundary lies the metastable region, where phase separation requires more than small perturbations. In this metastable region, small fluctuations tend to remain stable. However, if fluctuations are sufficiently large, phase separation will occur through nucleation and growth rather than via spinodal decomposition. This reflects the distinct behaviors of systems near the spinodal and binodal boundaries, where larger fluctuations lead to nucleation-driven separation instead of the continuous phase change associated with spinodal decomposition. Figure 3.5 shows the binodal simulations for alpha -0.5(a), as we can see small fluctuations (b) are not enough for a phase separation between binodal and spinodal lines (metastable region).

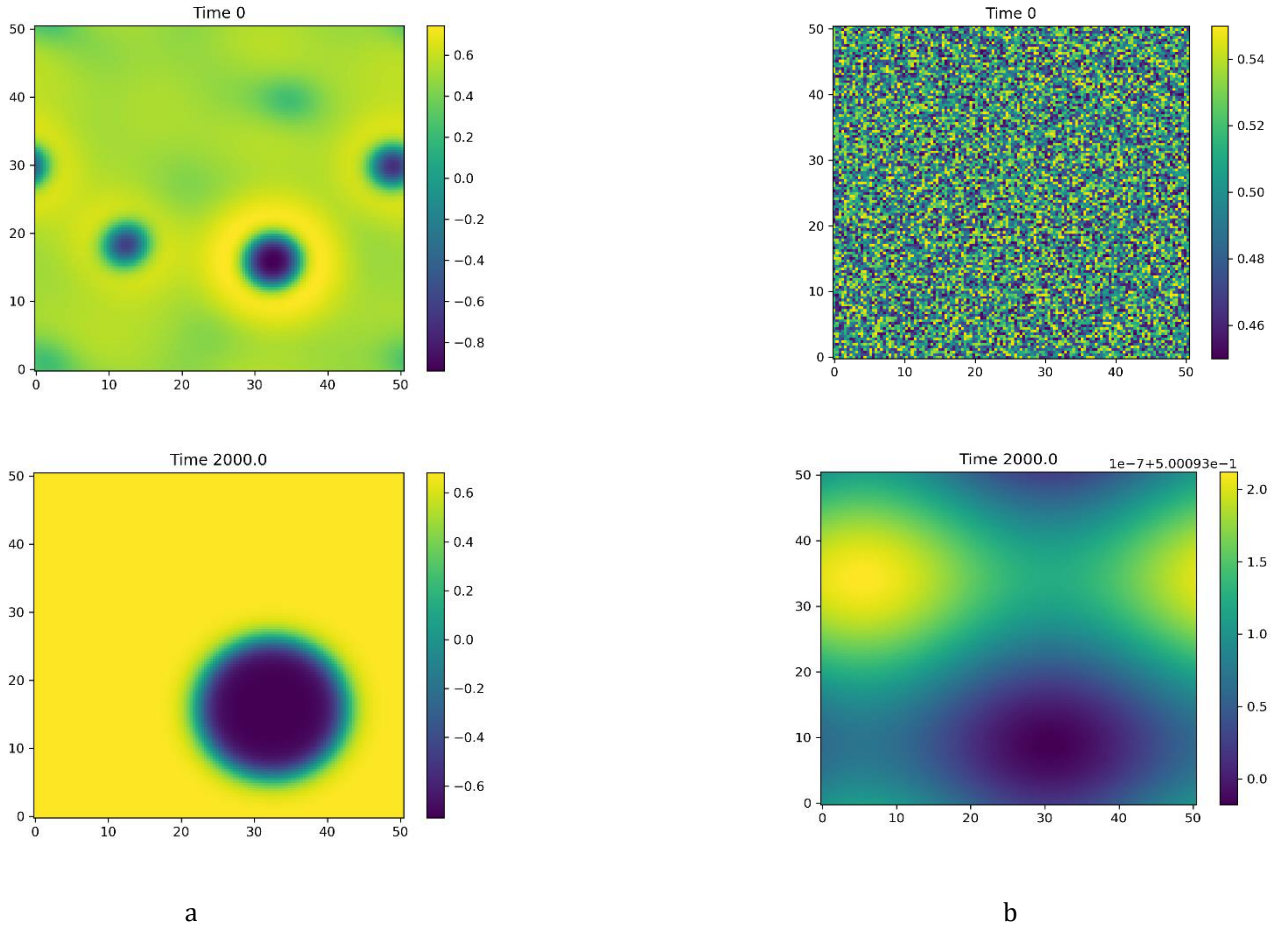

Figure 3.5 Simulation results for binodal, a) alpha= -0.5, b) small fluctuations

To analyze the spatial organization during the early stages of phase separation, we calculate the structure factor S(q), which provides critical insights into the concentration fluctuations across different spatial scales. The wave vector q, which is inversely related to spatial scale, while S(q) represents the intensity of these fluctuations. We calculate S(q) by performing the Fourier transform of the concentration field, averaged isotropically to capture the spatial correlations in all directions. At the first time step of the simulation, we observe the structure factor to identify the dominant wavelength of the emerging domains. We can calculate the peak of S(q) at a small q, which corresponds to the characteristic size of these initial domains. This peak reflects the primary length scale driven by the phase separation dynamics. As expected from the theoretical framework of the Cahn-Hilliard equation, the structure factor shows a sharp peak at smaller q values and a decay at higher q values, indicating that smaller-scale fluctuations are less significant.

This aligns with the fundamental prediction that phase separation leads to the growth of larger domains at the expense of smaller ones. To understand the domain size evolution more quantitatively, we calculate the characteristic domain length L(t) from S(q) using the equation 3.2:

(3.2) $$L(t) = \frac{\int S(q,t)\, dq}{\int qS(q,t)\, dq}$$

where the integrals are performed over the range of wave vectors (q) relevant to the system. This calculation allows us to track the growth of domains at any given time, providing a direct measure of how the system evolves spatially. By performing these calculations, we capture the initial spatial configuration of the system and lay the groundwork for understanding the subsequent coarsening process. The structure factor at the first time step serves as a crucial benchmark, offering a snapshot of the initial concentration fluctuations that will evolve into larger, more organized domains over time. This analysis not only validates the theoretical predictions of phase separation dynamics but also provides a robust method for monitoring the evolution of domain structures in numerical simulations. In practice, we compute S(q) using high-resolution grid data from our simulations, ensuring accurate representation of spatial fluctuations. The structure factor's behavior at the first time step is critical for understanding the onset of phase separation, and by calculating it precisely, we ensure a detailed comparison with theoretical models of domain growth and coarsening.

Figure 3.6 represents Domain Growth over Time, with time (t) on the x-axis and domain length (L(t)) on the y-axis, both plotted on logarithmic scales to highlight the scaling behavior. The blue dots indicate the measured or simulated data, showing the evolution of domain size during the coarsening process. The red dashed line represents a theoretical fit, following a power-law relation $L(t) \propto t^{\alpha}$, with the fitted growth exponent α=0.339. This exponent characterizes the rate of domain coarsening, reflecting the kinetics of phase separation. This behavior is consistent with the predictions of the Cahn-Hilliard equation, a theoretical framework that describes phase separation dynamics in binary mixtures. As the system undergoes spinodal decomposition, regions of distinct phases emerge and grow over time. The growth is driven by interfacial energy minimization and diffusion, leading to the characteristic scaling behavior shown in the graph. The fitted value of alpha = 0.339 suggests a growth rate slightly larger than the canonical α=1/3. This slight deviation might stem from specific system-dependent factors such as fluctuations, finite-size effects, or corrections due to hydrodynamic interactions. The agreement between the data points and the theoretical fit at long times emphasizes that the system reaches a universal scaling regime, where the growth is predominantly governed by curvature-driven coarsening. The graph effectively captures the universality of power-law scaling in domain growth, illustrating a key feature of phase separation and coarsening processes in a variety of physical and chemical systems, such as alloys, polymer blends, and even biological materials. This analysis provides crucial insights into the late-stage dynamics of phase separation, as described by the Cahn-Hilliard equation, showcasing the interplay between theory and numerical/experimental results.

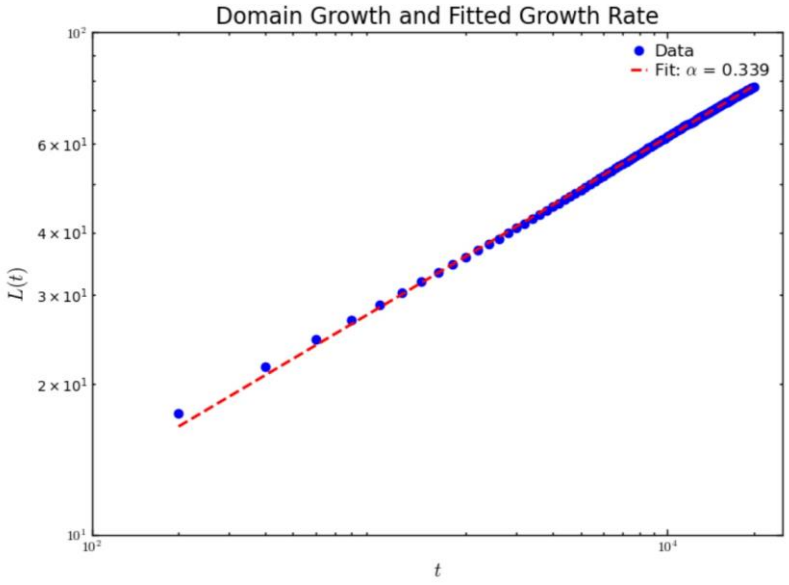

Figure 4.6 Domain growth and fitted growth rate

4. Conclusion

This comprehensive study of phase separation dynamics through the Cahn-Hilliard equation framework has yielded several significant insights into the behavior of binary mixtures. By combining theoretical analysis with numerical simulations, we have demonstrated the robust predictive power of the Cahn-Hilliard model in describing phase separation phenomena across various parameter regimes. Our investigation of interface profiles revealed strong agreement between theoretical predictions and numerical results, particularly in the scaling behavior of key parameters. The fitted values for parameters 'alpha' showed generally linear trends along expected values, though with some small deviations that highlight the complexities of numerical implementation. The state diagram analysis confirmed the theoretical predictions of linear stability analysis, with clear demarcation between phase-separated and non-phase-separated regions. The numerical simulations effectively captured the distinct behaviors in different regions of the phase diagram, including spinodal decomposition and nucleation-driven separation. Of particular interest was the observation of the critical points and phase boundaries, which aligned well with theoretical expectations derived from the Flory-Huggins theory. The temporal evolution of domain structures, as observed through our simulations, demonstrated classic coarsening behavior. The domain length growth followed a power law with an exponent of approximately 0.339, consistent with theoretical predictions for conserved order parameter systems. The structure factor analysis across different timesteps revealed characteristic scaling behaviors, providing valuable insights into the multi-scale nature of the phase separation process. Importantly, our results validate the use of the Cahn-Hilliard framework for modeling complex phase separation phenomena, while also highlighting its limitations and areas requiring careful consideration in numerical implementation. The study demonstrates that the combination of the Cahn-Hilliard equation with Flory-Huggins theory provides a powerful tool for understanding and predicting phase separation behavior in binary mixtures. These findings have significant implications for various applications, from materials science to biological systems. The validated numerical methods and analytical frameworks developed in this study can be applied to the design and optimization of material processing techniques, particularly in cases where controlled phase separation is desired. Future work could extend this analysis to more complex systems, including those with additional components or non-uniform mobility coefficients, and could investigate the effects of external fields or boundary conditions on phase separation dynamics. Understanding these fundamental processes of phase separation opens new possibilities for materials design and processing, potentially leading to improved methods for creating materials with desired microstructures and properties. The methodologies developed here provide a foundation for future investigations into more complex systems and phenomena in non-equilibrium thermodynamics.

References

1. Scherer, P. and S. Fischer, *Flory–Huggins Theory for Biopolymer Solutions*. 2017. p. 21-38.
2. Doi, M., *Soft Matter Physics*. 2013: Oxford University Press.
3. Papon, P., J. Leblond, and P.H. Meijer, *Physics of Phase Transitions*. 2002: Springer-Verlag Berlin Heidelberg, Germany.
4. L. Hecht, K.-R. Dormann, K. L. Spanheimer, M. Ebrahimi, M. Cordts, S. Mandal, A. K. Mukhopadhyay, and B. Liebchen, (2024).